

Initial Product-Ion Distributions in Ion-Molecule Reactions of CH_5^+ , C_2H_5^+ , and C_3H_5^+ with PhX ($X = \text{H}, \text{CH}_3, \text{C}_2\text{H}_5, \text{C}_2\text{H}_3,$ and C_2H)

Tsuji, Masaharu

Institute for Materials Chemistry and Engineering, and Research and Education Center of Green Technology

ARIKAWA, Takeshi

Department of Applied Science for Electronics and Materials, Interdisciplinary Graduate School of Engineering, Kyushu University : Graduate Student

Uto, Keiko

Institute for Materials Chemistry and Engineering, and Research and Education Center of Green Technology

Hayashi, Jun-ichiro

Institute for Materials Chemistry and Engineering, and Research and Education Center of Green Technology

他

<https://doi.org/10.15017/2544160>

出版情報 : 九州大学大学院総合理工学報告. 41 (2), pp.1-11, 2020-02. Interdisciplinary Graduate School of Engineering Sciences, Kyushu University

バージョン :

権利関係 :

Initial Product-Ion Distributions in Ion-Molecule Reactions of CH_5^+ , C_2H_5^+ , and C_3H_5^+ with PhX (X = H, CH_3 , C_2H_5 , C_2H_3 , and C_2H)

Masaharu TSUJI^{*1,2†} Takeshi ARIKAWA^{*3} Keiko UTO^{*1}

Jun-Ichiro HAYASHI^{*1,2} and Takeshi TSUJI^{*4}

[†]E-mail of corresponding author: tsuji@cm.kyushu-u.ac.jp

(Received August 26, 2019, accepted September 9, 2019)

The gas-phase ion-molecule reactions of CH_5^+ , C_2H_5^+ , and C_3H_5^+ with five monosubstituted benzenes (M = PhX: X = H, CH_3 , C_2H_5 , C_2H_3 , and C_2H) have been investigated under a reactant-ion selective mode of an ion-trap type of GC/MS. The dependence of product-ion distributions on the reaction time indicated that collisional stabilization takes part in the formation of such adduct ions as (M + C_2H_5)⁺, (M + C_3H_5)⁺, and (M + $\text{C}_3\text{H}_5 - \text{C}_2\text{H}_4$)⁺. It was found that radiative association also participates in the formation of (M + C_3H_5)⁺ adduct ion for M = Ph C_2H . The initial product-ion distributions were determined by extrapolating the dependence of branching ratios of product ions on the reaction time to zero reaction time. The reaction mechanisms were discussed based on initial product-ion distributions and heats of reactions of each product channel estimated from semi-empirical quantum calculations.

Key words: *Hydrocarbon ions, Benzene derivatives, Aromatic hydrocarbons, Chemical ionization, Ion trap type GC/MS, Collisional stabilization, Radiative association*

1. Introduction

We have made a systematic mass-spectrometric study on ion-molecule reactions of such typical hydrocarbon ions as CH_5^+ , C_2H_5^+ , and C_3H_5^+ with mono-substituted benzenes using an ion-trap type of GC/MS.¹⁻⁷ In a previous paper for aromatic hydrocarbons, results for PhX (X = H and CH_3) have been reported.¹ The reaction mechanisms of these two typical aromatic hydrocarbons for the three hydrocarbon ions were discussed based on product-ion distributions and heats of reactions in each product channel.

We discussed reaction mechanisms of PhX (X = H and CH_3) for CH_5^+ , C_2H_5^+ , and C_3H_5^+ ions on the basis of product-ion distributions measured at a constant reaction time of 20 ms, assuming that the effects of secondary collisions were

insignificant. However, we have noticed that this assumption is incorrect, because total number of collisions of a product ion with chemical ionization (CI) CH_4 gas is estimated to be about 50 times at 20 ms on the basis of a simple hard sphere gas kinetic model. Therefore, collisional stabilization may participate in the formation of product ions.

In the present study, we have reinvestigated the ion-molecule reactions of CH_5^+ , C_2H_5^+ , and C_3H_5^+ ions with PhX (X = H and CH_3). In addition, reactions with PhX (X = C_2H_5 , C_2H_3 , and C_2H) are investigated in order to obtain more detailed information on substitution effects of benzene mono-derivatives having saturated and unsaturated hydrocarbons. The dependence of product-ion distribution on the reaction time is measured in order to examine the contribution of collisional stabilization to the formation of each product ion. The initial product-ion distributions are estimated by extrapolating the dependence of branching ratios of product ions on the reaction time to zero reaction time. The reaction mechanisms are discussed based on initial product-ion distributions and thermochemical calculations

*1 Institute for Materials Chemistry and Engineering, and Research and Education Center of Green Technology

*2 Department of Applied Science for Electronics and Materials

*3 Department of Applied Science for Electronics and Materials, Graduate Student

*4 Department of Materials Science, Shimane University

of heats of reactions using a semi-empirical PM3 method.

2. Experimental

CH_4 CI mass spectra were obtained using an ion-trap type of Hitachi M7200 GC/MS in a reactant-ion selective mode. The electron-impact ionization on CH_4 provides primary CH_n^+ ($n = 2-4$) ions, and the subsequent fast ion-molecule reactions yield the secondary CH_5^+ , C_2H_5^+ , and C_3H_5^+ ions with chemical structures given in Fig. 1:⁸⁾

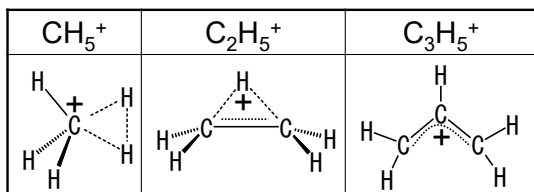
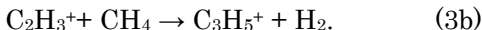
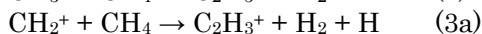
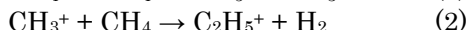
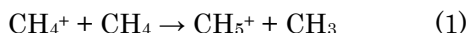


Fig. 1. Chemical structures of CH_5^+ , C_2H_5^+ , and C_3H_5^+ ions.

Since further reactions of CH_5^+ , C_2H_5^+ , and C_3H_5^+ with CH_4 are very slow, these ions become dominant reactant ions in the CH_4 CI experiments. The reactant CH_5^+ , C_2H_5^+ , or C_3H_5^+ ion was selectively trapped in the ion trap. The maximum and average kinetic energies of the reactant ions in our apparatus

were evaluated to be 10 and 4.2 eV for CH_5^+ , 6.0 and 2.4 eV for C_2H_5^+ , and 4.3 and 1.7 eV for C_3H_5^+ , respectively, using a pseudo-potential well method.⁹⁾ These energies are higher than that in the medium-pressure CI experiments, which was estimated to be less than 1 eV.¹⁰⁾

The time for storing a reactant ion was 5 ms. The reaction time was varied from 1 to 100 ms. The ion-trap cell was kept at ≤ 170 °C. The reagents were diluted in hexane and injected into the GC with a high-purity carrier He gas. The partial pressures of He and CH_4 in an ion-trap cell were estimated to be 5×10^{-5} and 7×10^{-5} Torr, respectively. The mass spectra were measured at low reagent concentrations of about 1000–10000 pg cm^{-3} in order to remove secondary ion-molecule reactions with reagent molecules.

3. Results and discussion

3.1 Summary of Mass Spectroscopic Data

The observed product ions, their reaction-time dependence, and initial product-ion distributions in each reaction are summarized in Table 1. The branching ratios of product ions either increase, decrease, or unchanged with increasing the reaction time. They are represented by +, −, and 0, respectively, in brackets in Table 1. The initial product-ion distributions were estimated by extrapolating the dependence of branching ratios of product ions on the reaction time to zero reaction time. The uncertainties of the branching ratios were estimated to be within $\pm 7\%$.

Table 1. Branching ratios (%) of product ions produced from reactions of CH_5^+ , C_2H_5^+ , and C_3H_5^+ ions with PhX (X = H, CH_3 , C_2H_5 , C_2H_3 , and C_2H).^{a)}

Reagents Reactant ions	PhH			PhCH ₃			PhC ₂ H ₅			PhC ₂ H ₃			PhC ₂ H		
	CH ₅ ⁺	C ₂ H ₅ ⁺	C ₃ H ₅ ⁺	CH ₅ ⁺	C ₂ H ₅ ⁺	C ₃ H ₅ ⁺	CH ₅ ⁺	C ₂ H ₅ ⁺	C ₃ H ₅ ⁺	CH ₅ ⁺	C ₂ H ₅ ⁺	C ₃ H ₅ ⁺	CH ₅ ⁺	C ₂ H ₅ ⁺	C ₃ H ₅ ⁺
Product ions															
(M + H) ⁺	100	100	66(+)	100	100	71(-)	58(+)	100	48(-)	100	83(-)	44(-)	100	92(-)	49(-)
(M + H - CH ₄) ⁺							0(+)								
(M + H - C ₂ H ₄) ⁺							42(-)								
(M + C ₂ H ₅) ⁺										0(+)			0(+)		
(M + C ₂ H ₅ - C ₃ H ₄) ⁺													8(+)		
(M + C ₂ H ₅ - C ₃ H ₆) ⁺										17(-)					
(M + C ₃ H ₅) ⁺						0(+)		0(+)				0(+)			6(+)
(M + C ₃ H ₅ - CH ₃) ⁺															35(+)
(M + C ₃ H ₅ - C ₂ H ₄) ⁺			34(-)			26(+)		40(+)				0(+)			4(-)
(M + C ₃ H ₅ - C ₄ H ₄) ⁺															6(-)
(M + C ₃ H ₅ - C ₄ H ₆) ⁺												56(-)			
(M - H) ⁺						3(+)		12(0)							

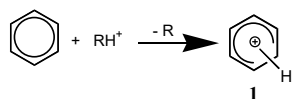
^{a)} Symbols, +, −, and 0 in brackets denote its branching ratio increases, decreases, or unchanged with increasing the reaction time, respectively.

3.2 Benzene (PhH)

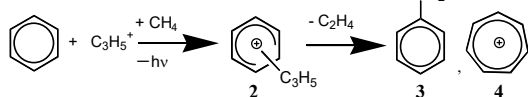
In the CH_5^+/PhH and $\text{C}_2\text{H}_5^+/\text{PhH}$ reactions, only $(\text{M} + \text{H})^+$ ion is observed. In the $\text{C}_3\text{H}_5^+/\text{PhH}$ reaction, besides a major $(\text{M} + \text{H})^+$ ion with a branching ratio of 66%, $(\text{M} + \text{C}_3\text{H}_5 - \text{C}_2\text{H}_4)^+$ ion is observed as a minor ion (34%). Possible reaction pathways for the RH^+/PhH reactions are shown in Scheme 1. Collisional stabilization and radiative association can participate in the association reactions. They are shown using such symbols as $+\text{CH}_4$ and $-\text{h}\nu$, respectively, in Scheme 1.

The $(\text{M} + \text{H})^+$ ion is formed through proton transfer (PT) [Scheme (1a)], which are 0.05–2.16 eV exothermic on the basis of energy calculations (Table A1 (Appendix)). In general, the proton-donating ability (acidity) of hydrocarbon ions decreases with increasing the dissociation energy of $\text{RH}^+ \rightarrow \text{R} + \text{H}^+$, which is denoted as $D_0(\text{R}-\text{H}^+)$. Since the $D_0(\text{R}-\text{H}^+)$ value increases in the order of CH_5^+ (5.7 eV), C_2H_5^+ (7.1 eV), and C_3H_5^+ (7.83 eV for $\text{CH}_2=\text{CHCH}_2^+$),¹¹⁾ the acidity of hydrocarbon ions decreases in the same order. One reason for the small branching ratio of the PT channel in the $\text{C}_3\text{H}_5^+/\text{PhH}$ reaction is the weakest acidity of the C_3H_5^+ ion.

(1a) Protonation



(1b) Association



Scheme 1. Possible reaction pathways for the ion-molecule reactions of RH^+ ($\text{R} = \text{CH}_4$, C_2H_4 , and C_3H_4) with PhH.

In order to examine the contribution of collisional stabilization, the dependence of product-ion distributions on the reaction time was measured in the $\text{C}_3\text{H}_5^+/\text{PhH}$ reaction (Fig. 2). The branching ratio of $(\text{M} + \text{C}_3\text{H}_5 - \text{C}_2\text{H}_4)^+$ ion decreases with increasing the reaction time. This indicates that collisional stabilization does not participate in the formation of $(\text{M} + \text{C}_3\text{H}_5 - \text{C}_2\text{H}_4)^+$. In general, effects of collisional stabilization is small for PT reactions. However, an increase in the branching ratio of $(\text{M} + \text{H})^+$ ion with increasing the reaction time suggests that collisions with CI CH_4 gas slightly contributes to the formation of $(\text{M} + \text{H})^+$ ion in the $\text{C}_3\text{H}_5^+/\text{PhH}$ reaction.

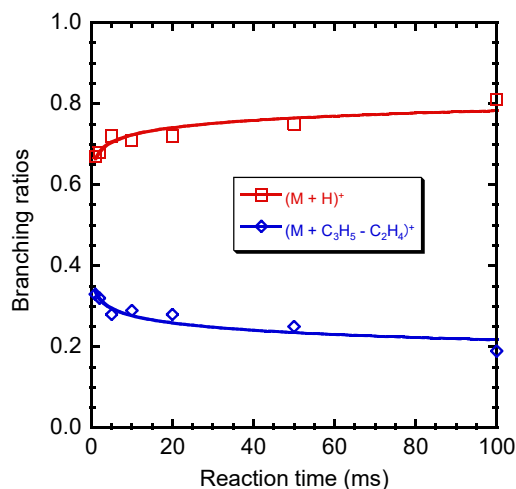


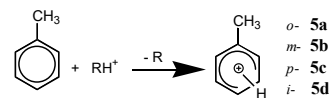
Fig. 2. Dependence of branching ratios of product ions on the reaction time in the $\text{C}_3\text{H}_5^+/\text{PhH}$ reaction.

The $(\text{M} + \text{C}_3\text{H}_5 - \text{C}_2\text{H}_4)^+$ ion is produced through dissociative association by loss of C_2H_4 [Scheme (1b)]. There are two possible products for $(\text{M} + \text{C}_3\text{H}_5 - \text{C}_2\text{H}_4)^+$ ion as shown in 3 (PhCH_2^+) and 4 (C_7H_7^+) in Scheme (1b). On the basis of energy calculations (Table A1 (Appendix)), the heat of reaction for the formation of 4 (C_7H_7^+) is lower than that of 3 (PhCH_2^+) by 0.53 eV. Therefore, 4 (C_7H_7^+) will be a major product ion as $(\text{M} + \text{C}_3\text{H}_5 - \text{C}_2\text{H}_4)^+$.

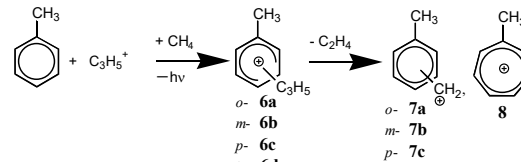
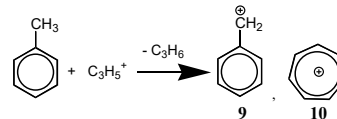
3.3 Toluene (PhCH₃)

Only PT channel leading to $(\text{M} + \text{H})^+$ [Scheme (2a)] is found in the $\text{CH}_5^+/\text{PhCH}_3$ and $\text{C}_2\text{H}_5^+/\text{PhCH}_3$ reactions. It should be noted that in addition to the $(\text{M} + \text{H})^+$ ion, $(\text{M} + \text{C}_3\text{H}_5)^+$ and

(2a) Protonation



(2b) Association

(2c) H⁻ Abstraction

Scheme 2. Possible reaction pathways for the ion-molecule reactions of RH^+ ($\text{R} = \text{CH}_4$, C_2H_4 , and C_3H_4) with PhCH_3 .

$(\text{M} + \text{C}_3\text{H}_5 - \text{C}_2\text{H}_4)^+$ ions arising from association reactions [Scheme (2b)] and $(\text{M} - \text{H})^+$ ion resulting from the hydride ion abstraction reaction [Scheme (2c)] are observed in the $\text{C}_3\text{H}_5^+/\text{PhCH}_3$ reaction.

It is known that three-body collisional association and two-body radiative association can participate in the formation of adduct ions.^{12,13} In radiative association, adduct ions are stabilized by radiating infrared emissions. A typical rate of infrared emission would be $100 \text{ photons s}^{-1}$, whereas the total collision numbers in this study are estimated to be 2–240 times during reaction times of 1–100 ms, corresponding to the collision rate of $2400 \text{ collisions s}^{-1}$. Therefore, not only radiative association ($-\text{h}\nu$) but also collisional association ($+\text{CH}_4$) may participate in the formation of $(\text{M} + \text{C}_3\text{H}_5)^+$ under our operating conditions.

Fig. 3 shows the dependence of branching ratios of product ions on the reaction time in the $\text{C}_3\text{H}_5^+/\text{PhCH}_3$ reaction. The branching ratios of $(\text{M} + \text{C}_3\text{H}_5)^+$ and $(\text{M} + \text{C}_3\text{H}_5 - \text{C}_2\text{H}_4)^+$ ions increase, as the reaction time increases. These results imply that collisional stabilization takes part in the formation of $(\text{M} + \text{C}_3\text{H}_5)^+$ and $(\text{M} + \text{C}_3\text{H}_5 - \text{C}_2\text{H}_4)^+$ ions. The disappearance of $(\text{M} + \text{C}_3\text{H}_5)^+$ ion at zero reaction time indicates that this adduct ion is exclusively produced by collisional stabilization and radiative association does not contribute to the formation of $(\text{M} + \text{C}_3\text{H}_5)^+$. The branching ratio of the $(\text{M} - \text{H})^+$ ion slightly increases with increasing the reaction time, suggesting that collisional stabilization takes part in the formation of $(\text{M} - \text{H})^+$.

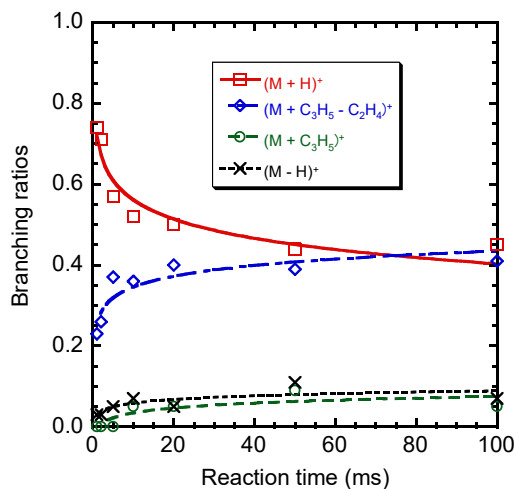
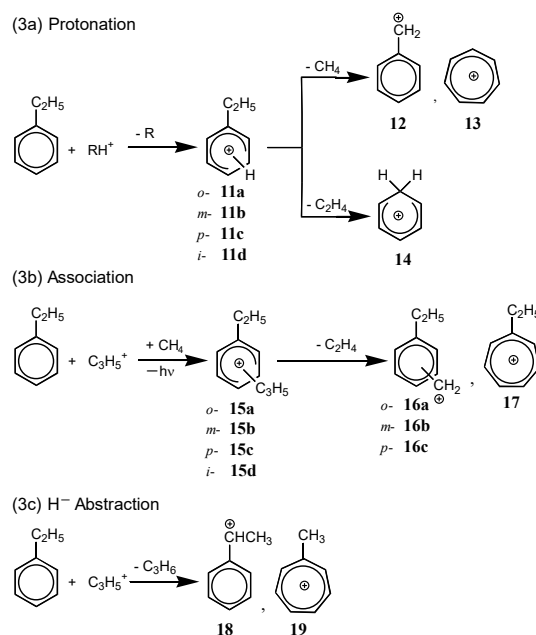


Fig. 3. Dependence of branching ratios of product ions on the reaction time in the $\text{C}_3\text{H}_5^+/\text{PhCH}_3$ reaction.

The major $(\text{M} + \text{H})^+$ ions (5a–5d) with branching ratios of 71–100% are formed through an attack on the benzene ring [Scheme (2a)]. Minor $(\text{M} + \text{C}_3\text{H}_5 - \text{C}_2\text{H}_4)^+$ and $(\text{M} - \text{H})^+$ ions with branching ratios of 26 and 3%, respectively, are formed through dissociative association [Scheme (2b)] and H^- abstraction [Scheme (2c)]. Molecular structures 7 and 8 are possible as $(\text{M} + \text{C}_3\text{H}_5 - \text{C}_2\text{H}_4)^+$ ions, whereas molecular structures 9 and 10 are possible as $(\text{M} - \text{H})^+$. On the basis of energy calculations given in Table A1 (Appendix), tropylium type ions 8 and 10 are energetically favorable products. Therefore, they will be dominant product ions.

3.4 Ethylbenzene (PhC_2H_5)

Major product channels for PhC_2H_5 is PT as in the cases of PhH and PhCH_3 [Scheme (3a)]. Although only non-dissociative PT channel is observed in the CH_5^+/PhH and $\text{CH}_5^+/\text{PhCH}_3$ reactions, not only non-dissociative PT channel (58%) but also dissociative PT channels leading to $(\text{M} + \text{H} - \text{CH}_4)^+$ and $(\text{M} + \text{H} - \text{C}_2\text{H}_4)^+$ (42%) are found in the $\text{CH}_5^+/\text{PhC}_2\text{H}_5$ reaction [Scheme (3a)]. In the $\text{C}_2\text{H}_5^+/\text{PhC}_2\text{H}_5$ and $\text{C}_3\text{H}_5^+/\text{PhC}_2\text{H}_5$ reactions, only non-dissociative PT channel is found. In the $\text{C}_3\text{H}_5^+/\text{PhC}_2\text{H}_5$ reaction, besides non-dissociative PT channel with a branching ratio of 48%, association reactions leading to $(\text{M} + \text{C}_3\text{H}_5)^+$ and $(\text{M} + \text{C}_3\text{H}_5 - \text{C}_2\text{H}_4)^+$ ions and H^- abstraction reaction leading to $(\text{M} - \text{H})^+$ ion are



Scheme 3. Possible reaction pathways for the ion-molecule reactions of RH^+ ($\text{R} = \text{CH}_4$, C_2H_4 , and C_3H_4) with PhC_2H_5 .

observed with total branching ratios of 40 and 12%, respectively [Scheme (3b) and (3c)].

Figs. 4a and 4b show the dependence of branching ratios of product ions on the reaction time in the $\text{CH}_5^+/\text{PhC}_2\text{H}_5$ and $\text{C}_3\text{H}_5^+/\text{PhC}_2\text{H}_5$ reactions, respectively. In the $\text{CH}_5^+/\text{PhC}_2\text{H}_5$ reaction, the branching ratios of $(\text{M} + \text{H})^+$ and $(\text{M} + \text{H} - \text{CH}_4)^+$ increase, whereas that of $(\text{M} + \text{H} - \text{C}_2\text{H}_4)^+$ decreases with increasing the reaction time. These results imply that collisional stabilization take part in the formation of the former ions. At zero reaction time, the branching ratio of $(\text{M} + \text{H} - \text{CH}_4)^+$ is zero, indicating that it is exclusively formed via collisional stabilization.

In the $\text{C}_3\text{H}_5^+/\text{PhC}_2\text{H}_5$ reaction, the branching ratios of $(\text{M} + \text{C}_3\text{H}_5)^+$ and $(\text{M} + \text{C}_3\text{H}_5 - \text{C}_2\text{H}_4)^+$ ions increase with increasing the reaction time. Although the branching ratio of the $(\text{M} + \text{C}_3\text{H}_5)^+$ ion decreases to zero as the reaction time decreases to zero, that of the $(\text{M} + \text{C}_3\text{H}_5 - \text{C}_2\text{H}_4)^+$ ion converges into a high value of 40% at zero

reaction time. On the basis of these findings, it was concluded that the adduct $(\text{M} + \text{C}_3\text{H}_5)^+$ ion is produced only through collisional stabilization, whereas most of the $(\text{M} + \text{C}_3\text{H}_5 - \text{C}_2\text{H}_4)^+$ ion is formed through without the contribution of collisional stabilization.

In Scheme 3 are shown observed major reaction pathways of the $\text{RH}^+/\text{PhC}_2\text{H}_5$ reactions. The $(\text{M} + \text{H})^+$, $(\text{M} + \text{H} - \text{CH}_4)^+$, $(\text{M} + \text{H} - \text{C}_2\text{H}_4)^+$, $(\text{M} + \text{C}_3\text{H}_5)^+$, and $(\text{M} + \text{C}_3\text{H}_5 - \text{C}_2\text{H}_4)^+$ ions are formed through electrophilic attack on the benzene ring [Scheme (3a) and (3b)], whereas $(\text{M} - \text{H})^+$ ion is formed by H^- abstraction from the C_2H_5 group [Scheme (3c)]. The chemical structure of $(\text{M} + \text{C}_3\text{H}_5 - \text{C}_2\text{H}_4)^+$ is 14. Two chemical structures, 12 and 13, 16 and 17, and 18 and 19, are possible for the $(\text{M} + \text{H} - \text{CH}_4)^+$, $(\text{M} + \text{C}_3\text{H}_5 - \text{C}_2\text{H}_4)^+$, and $(\text{M} - \text{H})^+$ ions, respectively. In all cases, tropylium type ions 13, 17, and 19 are more favorable on the basis of energy calculations (Table A1 (Appendix)). It is therefore reasonable to assume that these are major product ions.

3.5 Styrene (PhC_2H_3)

Only PT reaction [Scheme (4a)] is observed in the $\text{CH}_5^+/\text{PhC}_2\text{H}_3$ reaction. In the $\text{C}_2\text{H}_5^+/\text{PhC}_2\text{H}_3$ reaction, the dominant product channel (83%) is PT. In addition, association reactions leading to $(\text{M} + \text{C}_2\text{H}_5)^+$ and $(\text{M} + \text{C}_2\text{H}_5 - \text{C}_3\text{H}_6)^+$ ions are observed with a total branching ratio of 17% [Scheme (4b)]. In the $\text{C}_3\text{H}_5^+/\text{PhC}_2\text{H}_3$ reaction, the dominant product channel (56%) is the dissociative association leading to $(\text{M} + \text{C}_3\text{H}_5 - \text{C}_4\text{H}_6)^+$ ion, and the rest of the product channel (44%) is PT.

Figs. 5a and 5b show the branching ratios of product ions on the reaction time in the $\text{C}_2\text{H}_5^+/\text{PhC}_2\text{H}_3$ and $\text{C}_3\text{H}_5^+/\text{PhC}_2\text{H}_3$ reactions, respectively. In Fig. 5a, the branching ratio of $(\text{M} + \text{C}_2\text{H}_5)^+$ increases with increasing the reaction time. Its branching ratio becomes zero at zero reaction time, indicating that $(\text{M} + \text{C}_2\text{H}_5)^+$ is selectively formed by collisional stabilization. In Fig. 5b, the branching ratio of $(\text{M} + \text{C}_3\text{H}_5 - \text{C}_4\text{H}_6)^+$ slightly decreases with increasing the reaction time. Therefore, most of this ion is formed without effects of collisional stabilization. Although other association channels leading to $(\text{M} + \text{C}_3\text{H}_5)^+$ and $(\text{M} + \text{C}_3\text{H}_5 - \text{C}_2\text{H}_4)^+$ are found in the $\text{C}_3\text{H}_5^+/\text{PhC}_2\text{H}_3$ reaction, their branching ratios are zero at zero reaction time. On the basis of these findings, the adduct $(\text{M} + \text{C}_3\text{H}_5)^+$ and $(\text{M} + \text{C}_3\text{H}_5 - \text{C}_2\text{H}_4)^+$

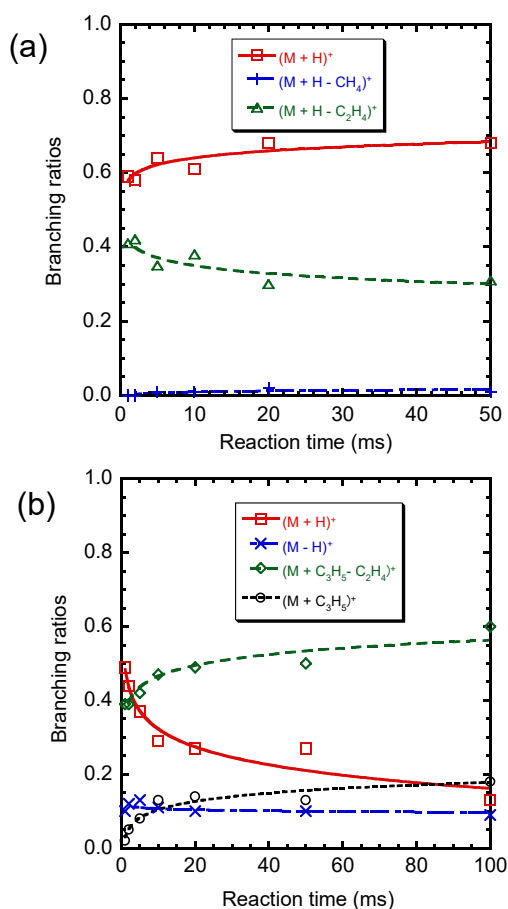
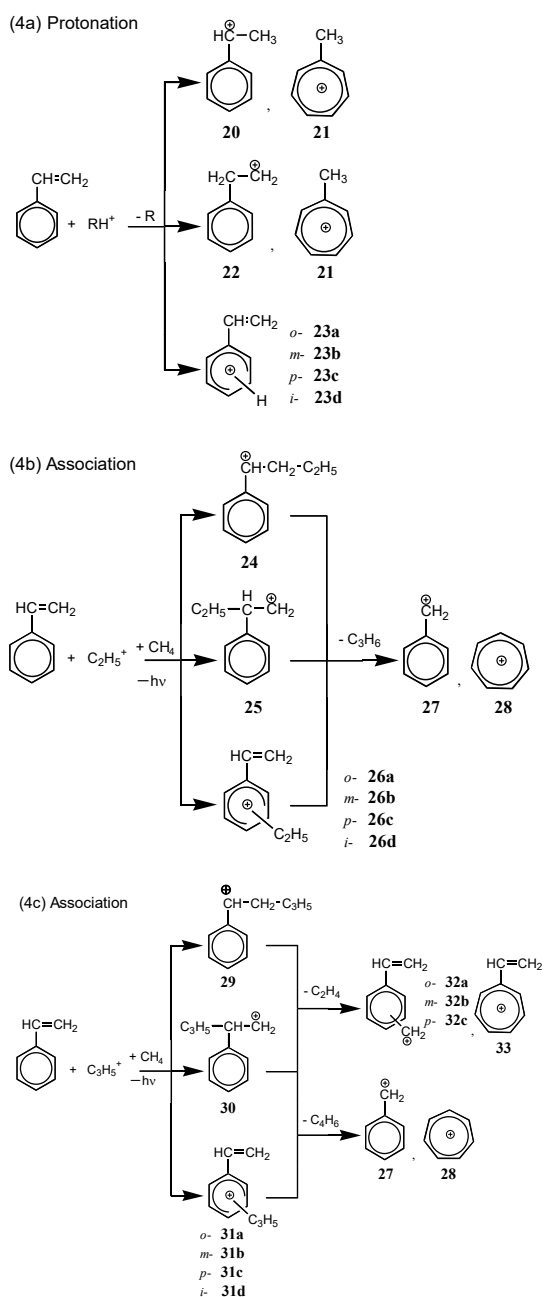


Fig. 4. Dependence of branching ratios of product ions on the reaction time in the (a) $\text{CH}_5^+/\text{PhC}_2\text{H}_5$ and (b) $\text{C}_3\text{H}_5^+/\text{PhC}_2\text{H}_5$ reactions.



Scheme 4. Possible reaction pathways for the ion-molecule reactions of RH^+ ($R = CH_4, C_2H_4,$ and C_3H_4) with PhC_2H_3 .

ions are produced only through collisional stabilization.

In Scheme (4a)–(4c) are shown the observed major reaction pathways of the RH^+/PhC_2H_3 reactions. The $(M + H)^+$, $(M + C_2H_5)^+$, $(M + C_2H_5 - C_3H_6)^+$, $(M + C_3H_5)^+$, $(M + C_3H_5 - C_2H_4)^+$, and $(M + C_3H_5 - C_4H_6)^+$ ions are formed through electrophilic attack on the benzene ring and/or the vinyl group. On the basis of energy diagram of these products (Table A1 (Appendix)),

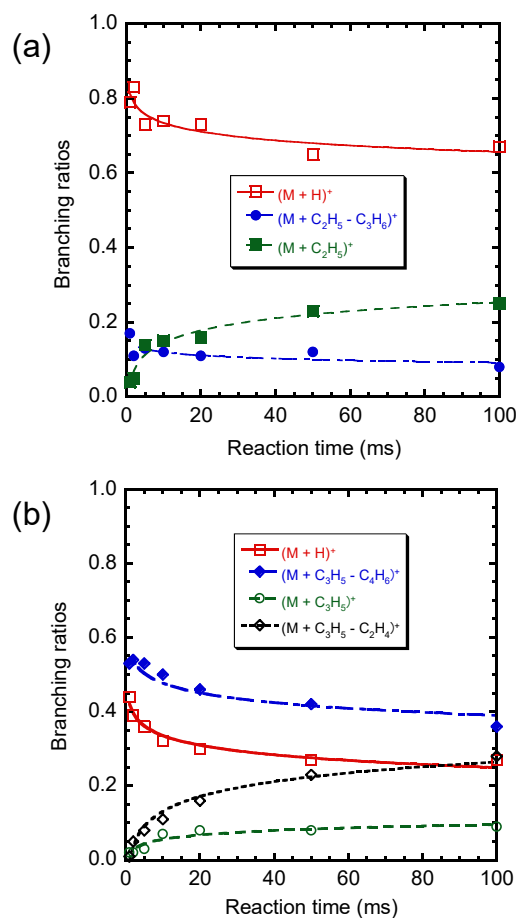
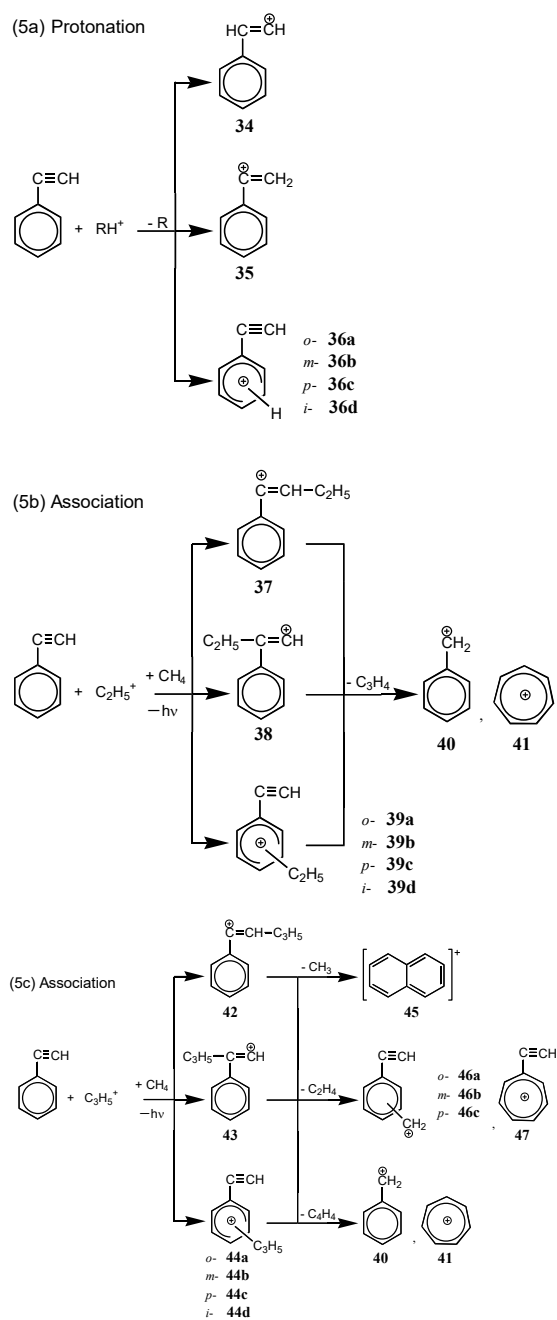


Fig. 5. Dependence of branching ratios of product ions on the reaction time in the (a) $C_2H_5^+/PhC_2H_3$ and (b) $C_3H_5^+/PhC_2H_3$ reactions.

electrophilic attack of H^+ , $C_2H_5^+$, and $C_3H_5^+$ on the vinyl group is favorable. Therefore, tropylium type ions, 21 in Scheme (4a), 28 in Scheme (4b), and 33 and 28 in Scheme (4c) formed via electrophilic attack of reactant ions on the vinyl group will be dominant products. In Scheme (4a), (4b), and (4c), chemical structures 20, 25, and 30 are more stable than 22, 24, and 29. Therefore, they will be major initial protonated and adduct ions before isomerization and elimination of C_3H_6 , C_2H_4 , and C_4H_6 .

3.6 Phenylacetylene (PhC_2H)

Only PT reaction is observed in the CH_5^+/PhC_2H reaction [Scheme (5a)]. In the $C_2H_5^+/PhC_2H$ reaction, the major product channel (92%) is also PT. In addition, $(M + C_2H_5)^+$ and $(M + C_2H_5 - C_3H_4)^+$ ions are observed as minor products. In the $C_3H_5^+/PhC_2H$ reaction, about half of the reaction (49%) is PT and the rest of the half



Scheme 5. Possible reaction pathways for the ion-molecule reactions of RH^+ ($\text{R} = \text{CH}_4$, C_2H_4 , and C_3H_4) with PhC_2H .

reaction (51%) is the non-dissociative and dissociative association leading to $(\text{M} + \text{C}_3\text{H}_5)^+$, $(\text{M} + \text{C}_3\text{H}_5 - \text{CH}_3)^+$, $(\text{M} + \text{C}_3\text{H}_5 - \text{C}_2\text{H}_4)^+$, and $(\text{M} + \text{C}_3\text{H}_5 - \text{C}_4\text{H}_4)^+$. Among them, the $(\text{M} + \text{C}_3\text{H}_5 - \text{C}_2\text{H}_4)^+$ ion is a dominant ion (35%).

Figs. 6a and 6b show the dependence of product ions on the reaction time in the $\text{C}_2\text{H}_5^+/\text{PhC}_2\text{H}$ and $\text{C}_3\text{H}_5^+/\text{PhC}_2\text{H}$ reactions, respectively. Although the branching ratio of $(\text{M} + \text{C}_2\text{H}_5)^+$ ion increases with increasing the reaction time, it is zero at zero reaction time.

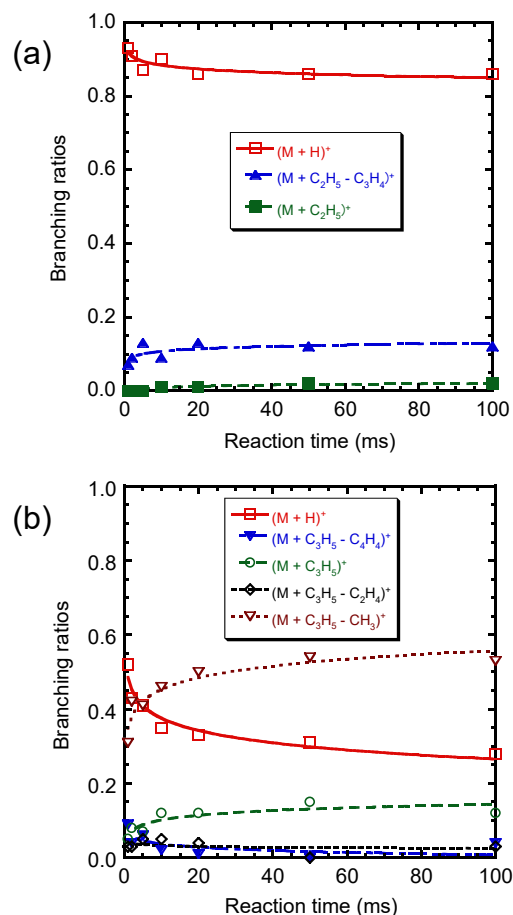


Fig. 6. Dependence of branching ratios of product ions on the reaction time in the (a) $\text{C}_2\text{H}_5^+/\text{PhC}_2\text{H}$ and (b) $\text{C}_3\text{H}_5^+/\text{PhC}_2\text{H}$ reactions.

Therefore the $(\text{M} + \text{C}_2\text{H}_5)^+$ ion is exclusively formed through the collisional stabilization. The branching ratio of $(\text{M} + \text{C}_2\text{H}_5 - \text{C}_3\text{H}_4)^+$ at zero reaction time is 8%, indicating that this ion is formed without assistance of collisional stabilization. Fig. 6b indicates that the collisional stabilization takes part in the formation of $(\text{M} + \text{C}_3\text{H}_5)^+$ and $(\text{M} + \text{C}_3\text{H}_5 - \text{CH}_3)^+$ ions. It should be noted that the branching ratio of $(\text{M} + \text{C}_3\text{H}_5)^+$ is not zero but 6% at zero reaction time. This implies that a small amount of $(\text{M} + \text{C}_3\text{H}_5)^+$ ion is formed through radiative association.

In Scheme 5 are shown the observed major reaction pathways of the $\text{RH}^+/\text{PhC}_2\text{H}$ reactions. The $(\text{M} + \text{H})^+$, $(\text{M} + \text{C}_2\text{H}_5)^+$, $(\text{M} + \text{C}_2\text{H}_5 - \text{C}_3\text{H}_4)^+$, $(\text{M} + \text{C}_3\text{H}_5)^+$, $(\text{M} + \text{C}_3\text{H}_5 - \text{CH}_3)^+$, $(\text{M} + \text{C}_3\text{H}_5 - \text{C}_2\text{H}_4)^+$, and $(\text{M} + \text{C}_3\text{H}_5 - \text{C}_4\text{H}_4)^+$ ions are formed through electrophilic attack on the benzene ring and/or the ethynyl group. On the basis of energy diagram of these product channels (Table A1 (Appendix)), electrophilic attack of H^+ , C_2H_5^+ , and C_3H_5^+ on the ethynyl group is

Table 2. Branching ratios (%) of each product channel in reactions of CH_5^+ , C_2H_5^+ , and C_3H_5^+ ions with PhX ($\text{X} = \text{H}, \text{CH}_3, \text{C}_2\text{H}_5, \text{C}_2\text{H}_3,$ and C_2H).

Reagents		PhH			PhCH ₃			PhC ₂ H ₅			PhC ₂ H ₃			PhC ₂ H		
Reactant ions		CH ₅ ⁺	C ₂ H ₅ ⁺	C ₃ H ₅ ⁺	CH ₅ ⁺	C ₂ H ₅ ⁺	C ₃ H ₅ ⁺	CH ₅ ⁺	C ₂ H ₅ ⁺	C ₃ H ₅ ⁺	CH ₅ ⁺	C ₂ H ₅ ⁺	C ₃ H ₅ ⁺	CH ₅ ⁺	C ₂ H ₅ ⁺	C ₃ H ₅ ⁺
Protonation	non-dissociative	100	100	66	100	100	71	58	100	48	100	83	44	100	92	49
	dissociative							42								
Association	non-dissociative															6
	dissociative			34			26			40		17	56		8	45
H ⁻ - Abstraction							3			12						

favorable. Therefore, major $(\text{M} + \text{H})^+$, $(\text{M} + \text{C}_2\text{H}_5)^+$, and $(\text{M} + \text{C}_3\text{H}_5)^+$ ions will be 35 in Scheme (5a), 37 in Scheme (5b), and 42 in Scheme (5c). Two chemical structures 40 and 41 are possible as $(\text{M} + \text{C}_3\text{H}_5 - \text{C}_3\text{H}_4)^+$. Since the formation of tropylium type ion 41 is energetically more favorable (Table A1 (Appendix)), it will be a dominant product. The $(\text{M} + \text{C}_3\text{H}_5 - \text{CH}_3)^+$ ion will be a stable naphthalene ion 45. Although two chemical structures 46 and 47 are possible as $(\text{M} + \text{C}_3\text{H}_5 - \text{C}_2\text{H}_4)^+$, whereas chemical structures 40 and 41 are possible as $(\text{M} + \text{C}_3\text{H}_5 - \text{C}_4\text{H}_4)^+$, more stable tropylium type ions 47 and 41 will be major product ions.

4. Summary and Conclusion

The gas-phase ion-molecule reactions of CH_5^+ , C_2H_5^+ , and C_3H_5^+ with five monosubstituted benzenes ($\text{M} = \text{PhX}$: $\text{X} = \text{H}, \text{CH}_3, \text{C}_2\text{H}_5, \text{C}_2\text{H}_3,$ and C_2H) have been investigated under a reactant-ion selective mode of an ion-trap type of GC/MS at a low CH_4 pressure. The dependence of product-ion distributions on the reaction time indicated that collisional stabilization takes part in the formation of such adduct ions as $(\text{M} + \text{C}_2\text{H}_5)^+$, $(\text{M} + \text{C}_3\text{H}_5)^+$, and $(\text{M} + \text{C}_3\text{H}_5 - \text{C}_2\text{H}_4)^+$. It was found that radiative association also participates in the formation of the $(\text{M} + \text{C}_3\text{H}_5)^+$ adduct ion for $\text{M} = \text{PhC}_2\text{H}$.

The branching ratios of protonation, association, and H^- abstraction are summarized in Table 2. In the CH_5^+ reactions, only PT was found. In the $\text{CH}_5^+/\text{PhC}_2\text{H}_5$ reaction, not only non-dissociative PT (58%) but also dissociative PT (42%) was observed. In the $\text{C}_2\text{H}_5^+/\text{PhX}$ ($\text{X} = \text{H}, \text{CH}_3, \text{C}_2\text{H}_5$) reactions, only non-dissociative PT was observed. In the $\text{C}_2\text{H}_5^+/\text{PhX}$ ($\text{X} = \text{C}_2\text{H}_3$ and C_2H) reactions, dominant product channel (83–92%) was also non-dissociative PT. In addition, small amounts of dissociative association channels (8–17%) leading to tropylium type ions were observed. The occurrence of association reactions in the $\text{C}_2\text{H}_5^+/\text{PhX}$ ($\text{X} = \text{C}_2\text{H}_3$ and C_2H) reactions can be attributed the fact that the

electrophilic attack of C_2H_5^+ on unsaturated C_2H_3 and C_2H groups is energetically favorable. In the C_3H_5^+ reactions, non-dissociative PT occupied 44–71%, and non-dissociative and dissociative association occupied 26–56%. In the $\text{C}_3\text{H}_5^+/\text{PhX}$ ($\text{X} = \text{CH}_3$ and C_2H_5) reactions, H^- abstraction channels were observed as minor processes (3–12%).

In all reactions, PT reactions were observed. For the cases of PhX ($\text{X} = \text{H}, \text{CH}_3,$ and C_2H_5), protonation occurs on a benzene ring. On the other hand, PT reactions can take place both on a benzene ring and a substituent for the cases of PhX ($\text{X} = \text{C}_2\text{H}_3$ and C_2H). On the basis of energetics, protonated ions formed by an attack on the substituent is more favorable. Therefore, PT reactions dominantly occur on the substituent.

References

- 1) M. Tsuji, E. Oda, and Y. Nishimura, *Chem. Lett.*, 26, 781 (1997).
- 2) M. Tsuji and Y. Nishimura, *Bull. Chem. Soc. Jpn.*, 71, 273 (1998).
- 3) M. Tsuji, K. Arikawa, and Y. Nishimura, *Bull. Chem. Soc. Jpn.*, 72, 293 (1999).
- 4) M. Tsuji, T. Arikawa, and Y. Nishimura, *Bull. Chem. Soc. Jpn.*, 73, 131 (2000).
- 5) M. Tsuji, T. Arikawa, Y. Tanaka, and Y. Nishimura, *Bull. Chem. Soc. Jpn.*, 73, 1673 (2000).
- 6) M. Tsuji, T. Arikawa, Y. Tanaka, K. Mogi, and Y. Sakai, *J. Mass Spectrom. Soc. Jpn.*, 49, 188 (2001).
- 7) T. Arikawa and M. Tsuji, *J. Mass Spectrom. Soc. Jpn.*, 59, 69 (2011).
- 8) F. H. Field and M. S. B. Munson, *J. Am. Chem. Soc.*, 87, 3289 (1965).
- 9) J. F. J. Todd, R. M. Waldren, and R. F. Bonner, *Int. J. Mass Spectrom. Ion Phys.*, 34, 17 (1980).
- 10) C. Chang, G. G. Meisels, and J. A. Taylor, *Int. J. Mass Spectrom. Ion Phys.*, 12, 411 (1973).
- 11) S. G. Lias, J. E. Bartmess, J. F. Liebman, J. L. Holmes, R. D. Levin, and W. G. Mallard, *J. Phys. Chem. Ref. Data*, 17, Suppl. 1 (1988); updated data were obtained from NIST Standard Ref. Database, Number 69, 2018 (<http://webbook.nist.gov/chemistry>).
- 12) R. C. Dunbar, *Int. J. Mass Spectrom. Ion Process.*, 100, 423 (1990).
- 13) G. Weddle and R. C. Dunbar, *Int. J. Mass Spectrom. Ion Process.*, 134, 73 (1994).

Appendix

Table A1. Heats of reactions of each product channel (in eV Units).^{a)}

Reactants	$\Sigma\Delta H^0$		Products	ΔH^0	Chemical structure ^{e)}
	Reactants	Products			
CH ₅ ⁺ + PhH	10.23	(M + H) ⁺ + CH ₄	8.07	-2.16	1
C ₂ H ₅ ⁺ + PhH	10.21	(M + H) ⁺ + C ₂ H ₄	9.39	-0.82	1
C ₃ H ₅ ⁺ + PhH	10.66	(M + H) ⁺ + C ₃ H ₄	10.61	-0.05	1
		(M + C ₃ H ₅) ⁺	9.89	-0.77	2
		(M + C ₃ H ₅) ⁺ = PhCH ₂ ⁺	9.87	-0.79	3
		(M + C ₃ H ₅) ⁺ = C ₇ H ₇ ⁺	9.34	-1.32	4
CH ₅ ⁺ + PhCH ₃	9.89	<i>σ</i> -(M + H) ⁺ + CH ₄	9.17	-0.70	5a
		<i>m</i> -(M + H) ⁺ + CH ₄	9.29	-0.58	5b
		<i>p</i> -(M + H) ⁺ + CH ₄	9.11	-0.76	5c
		<i>i</i> -(M + H) ⁺ + CH ₄	9.60	-0.27	5d
		(M + H) ⁺ (exp.) + CH ₄	8.69	-1.18	5
C ₂ H ₅ ⁺ + PhCH ₃	9.87	<i>σ</i> -(M + H) ⁺ + C ₂ H ₄	9.17	-0.70	5a
		<i>m</i> -(M + H) ⁺ + C ₂ H ₄	9.29	-0.58	5b
		<i>p</i> -(M + H) ⁺ + C ₂ H ₄	9.11	-0.76	5c
		<i>i</i> -(M + H) ⁺ + C ₂ H ₄	9.60	-0.27	5d
		(M + H) ⁺ (exp.) + C ₂ H ₄	8.69	-1.18	5
C ₃ H ₅ ⁺ + PhCH ₃	10.32	<i>σ</i> -(M + H) ⁺ + C ₃ H ₄	10.61	0.29	5a
		<i>m</i> -(M + H) ⁺ + C ₃ H ₄	10.73	0.41	5b
		<i>p</i> -(M + H) ⁺ + C ₃ H ₄	10.54	0.22	5c
		<i>i</i> -(M + H) ⁺ + C ₃ H ₄	11.04	0.72	5d
		(M + H) ⁺ (exp.) + C ₃ H ₄	10.13	-0.19	5
		<i>σ</i> -(M + C ₃ H ₅) ⁺	9.29	-1.03	6a
		<i>m</i> -(M + C ₃ H ₅) ⁺	9.43	-0.89	6b
		<i>p</i> -(M + C ₃ H ₅) ⁺	9.24	-1.08	6c
		<i>i</i> -(M + C ₃ H ₅) ⁺	9.82	-0.50	6d
		<i>σ</i> -CH ₃ C ₆ H ₄ CH ₂ ⁺ + C ₂ H ₄	9.92	-0.40	7a
		<i>m</i> -CH ₃ C ₆ H ₄ CH ₂ ⁺ + C ₂ H ₄	9.95	-0.37	7b
		<i>p</i> -CH ₃ C ₆ H ₄ CH ₂ ⁺ + C ₂ H ₄	9.80	-0.52	7c
		C ₇ H ₆ CH ₃ ⁺ + C ₂ H ₄	9.63	-0.69	8
		PhCH ₂ ⁺ + C ₃ H ₆	9.53	-0.79	9
		C ₇ H ₇ ⁺ + C ₃ H ₆	9.01	-1.31	10
CH ₅ ⁺ + PhC ₂ H ₅	9.67	<i>σ</i> -(M + H) ⁺ + CH ₄	7.67	-2.00	11a
		<i>m</i> -(M + H) ⁺ + CH ₄	7.80	-1.87	11b
		<i>p</i> -(M + H) ⁺ + CH ₄	7.59	-2.08	11c
		<i>i</i> -(M + H) ⁺ + CH ₄	8.04	-1.63	11d
		(M + H) ⁺ (exp.) + CH ₄	7.08	-2.59	11
		(M + H - CH ₄) ⁺ = PhCH ₂ ⁺	7.78	-1.89	12
		(M + H - CH ₄) ⁺ = C ₇ H ₇ ⁺	7.26	-2.41	13
		(M + H - C ₂ H ₄) ⁺ = PhH ₂ ⁺	8.62	-1.05	14
C ₂ H ₅ ⁺ + PhC ₂ H ₅	9.65	<i>σ</i> -(M + H) ⁺ + C ₂ H ₄	8.98	-0.67	11a
		<i>m</i> -(M + H) ⁺ + C ₂ H ₄	9.11	-0.54	11b
		<i>p</i> -(M + H) ⁺ + C ₂ H ₄	8.91	-0.74	11c
		<i>i</i> -(M + H) ⁺ + C ₂ H ₄	9.35	-0.30	11d
		(M + H) ⁺ (exp.) + C ₂ H ₄	8.39	-1.26	11
C ₃ H ₅ ⁺ + PhC ₂ H ₅	10.10	<i>σ</i> -(M + H) ⁺ + C ₃ H ₄	10.42	0.32	11a
		<i>m</i> -(M + H) ⁺ + C ₃ H ₄	10.55	0.45	11b
		<i>p</i> -(M + H) ⁺ + C ₃ H ₄	10.34	0.24	11c
		<i>i</i> -(M + H) ⁺ + C ₃ H ₄	10.79	0.69	11d
		(M + H) ⁺ (exp.) + C ₃ H ₄	9.83	-0.27	11
		<i>σ</i> -(M + C ₃ H ₅) ⁺	9.09	-1.01	15a

Table A1. Continued.

		$m\text{-(M + C}_3\text{H}_5)^+$	9.22	-0.88	15b
		$p\text{-(M + C}_3\text{H}_5)^+$	9.05	-1.05	15c
		$i\text{-(M + C}_3\text{H}_5)^+$	9.56	-0.54	15d
		$\sigma\text{-C}_2\text{H}_5\text{C}_6\text{H}_4\text{CH}_2^+ + \text{C}_2\text{H}_4$	9.75	-0.35	16a
		$m\text{-C}_2\text{H}_5\text{C}_6\text{H}_4\text{CH}_2^+ + \text{C}_2\text{H}_4$	9.78	-0.32	16b
		$p\text{-C}_2\text{H}_5\text{C}_6\text{H}_4\text{CH}_2^+ + \text{C}_2\text{H}_4$	9.61	-0.49	16c
		$\text{C}_7\text{H}_6\text{C}_2\text{H}_5^+ + \text{C}_2\text{H}_4$	9.49	-0.61	17
		$\text{PhCHCH}_3^+ + \text{C}_3\text{H}_6$	9.41	-0.69	18
		$\text{C}_7\text{H}_6\text{CH}_3^+ + \text{C}_3\text{H}_6$	9.29	-0.81	19
$\text{CH}_5^+ + \text{PhC}_2\text{H}_3$	10.90	PhCHCH_3^+	8.43	-2.47	20
		$\text{C}_7\text{H}_6\text{CH}_3^+$	8.31	-2.59	21
		$\text{PhCH}_2\text{CH}_2^+$	9.82	-1.08	22
		$\sigma\text{(M + H)}^+ + \text{CH}_4$	8.81	-2.09	23a
		$m\text{(M + H)}^+ + \text{CH}_4$	9.06	-1.84	23b
		$p\text{(M + H)}^+ + \text{CH}_4$	8.76	-2.14	23c
		$i\text{(M + H)}^+ + \text{CH}_4$	9.39	-1.51	23d
		$(\text{M + H})^+(\text{exp.}) + \text{CH}_4$	8.03	-2.87	23
$\text{C}_2\text{H}_5^+ + \text{PhC}_2\text{H}_3$	10.88	$\text{PhCHCH}_3^+ + \text{C}_2\text{H}_4$	9.74	-1.14	20
		$\text{C}_7\text{H}_6\text{CH}_3^+ + \text{C}_2\text{H}_4$	9.63	-1.25	21
		$\text{PhCH}_2\text{CH}_2^+ + \text{C}_2\text{H}_4$	11.13	0.25	22
		$\sigma\text{(M + H)}^+ + \text{C}_2\text{H}_4$	10.12	-0.76	23a
		$m\text{(M + H)}^+ + \text{C}_2\text{H}_4$	10.38	-0.50	23b
		$p\text{(M + H)}^+ + \text{C}_2\text{H}_4$	10.08	-0.80	23c
		$i\text{(M + H)}^+ + \text{C}_2\text{H}_4$	10.70	-0.18	23d
		$(\text{M + H})^+(\text{exp.}) + \text{C}_2\text{H}_4$	9.34	-1.54	23
		$\text{PhCHCH}_2\text{C}_2\text{H}_5^+$	8.67	-2.21	24
		$\text{PhCH}(\text{C}_2\text{H}_5)\text{CH}_2^+$	8.38	-2.50	25
		$\sigma\text{(M + C}_2\text{H}_5)^+$	9.19	-1.69	26a
		$m\text{(M + C}_2\text{H}_5)^+$	9.43	-1.45	26b
		$p\text{(M + C}_2\text{H}_5)^+$	9.13	-1.75	26c
		$i\text{(M + C}_2\text{H}_5)^+$	9.88	-1.00	26d
		$\text{PhCH}_2^+ + \text{C}_3\text{H}_6$	9.53	-1.35	27
		$\text{C}_7\text{H}_7^+ + \text{C}_3\text{H}_6$	9.01	-1.87	28
$\text{C}_3\text{H}_5^+ + \text{PhC}_2\text{H}_3$	11.33	$\text{PhCHCH}_3^+ + \text{C}_3\text{H}_4$	11.18	-0.15	20
		$\text{C}_7\text{H}_6\text{CH}_3^+ + \text{C}_3\text{H}_4$	11.06	-0.27	21
		$\text{PhCH}_2\text{CH}_2^+ + \text{C}_3\text{H}_4$	12.57	1.24	22
		$\sigma\text{(M + H)}^+ + \text{C}_3\text{H}_4$	11.55	0.22	23a
		$m\text{(M + H)}^+ + \text{C}_3\text{H}_4$	11.81	0.48	23b
		$p\text{(M + H)}^+ + \text{C}_3\text{H}_4$	11.51	0.18	23c
		$i\text{(M + H)}^+ + \text{C}_3\text{H}_4$	12.14	0.81	23d
		$(\text{M + H})^+(\text{exp.}) + \text{C}_3\text{H}_4$	10.78	-0.55	23
		$\text{PhCHCH}_2\text{C}_3\text{H}_5^+$	9.78	-1.55	29
		$\text{PhCH}(\text{C}_3\text{H}_5)\text{CH}_2^+$	9.43	-1.90	30
		$\sigma\text{(M + C}_3\text{H}_5)^+$	10.28	-1.05	31a
		$m\text{(M + C}_3\text{H}_5)^+$	10.52	-0.81	31b
		$p\text{(M + C}_3\text{H}_5)^+$	10.22	-1.11	31c
		$i\text{(M + C}_3\text{H}_5)^+$	10.95	-0.38	31d
		$\sigma\text{-C}_2\text{H}_3\text{C}_6\text{H}_4\text{CH}_2^+ + \text{C}_2\text{H}_4$	10.87	-0.46	32a
		$m\text{-C}_2\text{H}_3\text{C}_6\text{H}_4\text{CH}_2^+ + \text{C}_2\text{H}_4$	11.04	-0.29	32b
		$p\text{-C}_2\text{H}_3\text{C}_6\text{H}_4\text{CH}_2^+ + \text{C}_2\text{H}_4$	10.80	-0.53	32c
		$\text{C}_7\text{H}_6\text{C}_2\text{H}_3^+ + \text{C}_2\text{H}_4$	10.66	-0.67	33
		$\text{PhCH}_2^+ + \text{C}_4\text{H}_6$	11.01	-0.32	27
		$\text{C}_7\text{H}_7^+ + \text{C}_4\text{H}_6$	10.49	-0.84	28
$\text{CH}_5^+ + \text{PhC}_2\text{H}$	12.53	$\text{PhCHCH}^+ + \text{CH}_4$	11.62	-0.91	34
		$\text{PhCCH}_2^+ + \text{CH}_4$	10.21	-2.32	35

Table A1. Continued.

		σ -(M + H) ⁺ + CH ₄	10.45	-2.08	36a
		m -(M + H) ⁺ + CH ₄	10.65	-1.88	36b
		p -(M + H) ⁺ + CH ₄	10.42	-2.11	36c
		i -(M + H) ⁺ + CH ₄	11.01	-1.52	36d
		(M + H) ⁺ (exp.) + CH ₄	9.59	-2.94	36
C ₂ H ₅ ⁺ + PhC ₂ H	12.51	PhCHCH ⁺ + C ₂ H ₄	12.94	0.43	34
		PhCCH ₂ ⁺ + C ₂ H ₄	11.52	-0.99	35
		σ -(M + H) ⁺ + C ₂ H ₄	11.77	-0.74	36a
		m -(M + H) ⁺ + C ₂ H ₄	11.96	-0.55	36b
		p -(M + H) ⁺ + C ₂ H ₄	11.73	-0.78	36c
		i -(M + H) ⁺ + C ₂ H ₄	12.32	-0.19	36d
		(M + H) ⁺ (exp.) + C ₂ H ₄	10.91	-1.60	36
		PhCCHC ₂ H ₅ ⁺	10.34	-2.17	37
		PhC(C ₂ H ₅)CH ⁺	11.84	-0.67	38
		σ -(M + C ₂ H ₅) ⁺	10.86	-1.65	39a
		m -(M + C ₂ H ₅) ⁺	11.02	-1.49	39b
		p -(M + C ₂ H ₅) ⁺	10.78	-1.73	39c
		i -(M + C ₂ H ₅) ⁺	11.44	-1.07	39d
		PhCH ₂ ⁺ + C ₃ H ₄	11.30	-1.21	40
C ₃ H ₅ ⁺ + PhC ₂ H	12.97	C ₇ H ₇ ⁺ + C ₂ H ₄	10.78	-1.73	41
		σ -(M + H) ⁺ + C ₃ H ₄	13.20	0.23	1
		m -(M + H) ⁺ + C ₃ H ₄	13.40	0.43	1
		p -(M + H) ⁺ + C ₃ H ₄	13.17	0.20	1
		i -(M + H) ⁺ + C ₃ H ₄	13.76	0.79	1
		(M + H) ⁺ (exp.) + C ₃ H ₄	12.34	-0.63	1
		PhCHCH ⁺ + C ₃ H ₄	14.37	1.40	34
		PhCCH ₂ ⁺ + C ₃ H ₄	12.96	-0.01	35
		PhCCHC ₃ H ₅ ⁺	11.44	-1.53	42
		PhC(C ₃ H ₅)CH ⁺	12.87	-0.10	43
		σ -(M + C ₃ H ₅) ⁺	11.95	-1.02	44a
		m -(M + C ₃ H ₅) ⁺	12.11	-0.86	44b
		p -(M + C ₃ H ₅) ⁺	11.87	-1.10	44c
		i -(M + C ₃ H ₅) ⁺	12.51	-0.46	44d
		naphthalene ⁺ + CH ₃	11.21	-1.76	45
		σ -C ₂ HC ₆ H ₄ CH ₂ ⁺ + C ₂ H ₄	12.50	-0.47	46a
		m -C ₂ HC ₆ H ₄ CH ₂ ⁺ + C ₂ H ₄	12.62	-0.35	46b
		p -C ₂ HC ₆ H ₄ CH ₂ ⁺ + C ₂ H ₄	12.44	-0.53	46c
		C ₇ H ₆ C ₂ H ⁺	12.26	-0.71	47
		PhCH ₂ ⁺ + CH ₂ CCCH ₂	12.92	-0.05	40
		C ₇ H ₇ ⁺ + CH ₂ CCCH ₂	12.40	-0.57	41
		PhCH ₂ ⁺ + CH ₂ CHCCH	12.49	-0.48	40
C ₇ H ₇ ⁺ + CH ₂ CHCCH	11.97	-1.00	41		

- a) The symbols σ , m , p , and i represent ortho-, meta-, para-, and ipso-adduct ions, respectively. Thermochemical data calculated using reliable experimental values for ions in Ref. 11 are shown by exp., and the other values for ions are calculated using a PM3 method. b) $\Delta H^0(\text{Reaction}) = \Sigma \Delta H^0(\text{Product}) - \Sigma \Delta H^0(\text{Reactant})$. (c) Chemical structures in Scheme 1–5.